AIAA-2002-2914

Application of Modern Design of Experiments to CARS Thermometry in a Supersonic Combustor

P.M. Danehy and R. DeLoach
NASA Langley Research Center, Hampton, VA

A.D. Cutler
The George Washington University, Hampton, VA

22nd AIAA Aerodynamic Measurement Technology and Ground Testing Conference
24-26 June 2002
St. Louis, Missouri

APPLICATION OF MODERN DESIGN OF EXPERIMENTS TO CARS THERMOMETRY IN A SUPERSONIC COMBUSTOR

P. M. Danehy* and R. DeLoach**
Instrumentation Systems Development Branch
MS 236, NASA Langley Research Center
Hampton, VA 23681-2199

A. D. Cutler#
The George Washington University
MS 335, NASA Langley Research Center
Hampton, VA 23681-2199

Abstract

We have applied formal experiment design and analysis to optimize the measurement of temperature in a supersonic combustor at NASA Langley Research Center. We used the coherent anti-Stokes Raman spectroscopy (CARS) technique to map the temperature distribution in the flowfield downstream of an 1160 K, Mach 2 freestream into which supersonic hydrogen fuel is injected at an angle of 30 degrees. CARS thermometry is inherently a single-point measurement technique; it was used to map the flow by translating the measurement volume through the flowfield. The method known as "Modern Design of Experiments" (MDOE) was used to estimate the data volume required, design the test matrix, perform the experiment, and analyze the resulting data. MDOE allowed us to match the volume of data acquired to the precision requirements of the customer. Furthermore, one aspect of MDOE, known as response surface methodology, allowed us to develop precise maps of the flowfield temperature, allowing interpolation between measurement points. An analytic function in two spatial variables was fit to the data from a single measurement plane. Fitting with a cosine series bivariate function allowed the mean temperature to be mapped with 95% confidence intervals of ±30 K, comfortably meeting the precision requirement of ±50 K specified prior to performing the experiments. We estimate that applying MDOE to the present experiment saved a factor of five in data volume acquired, compared to experiments executed in the traditional manner. Furthermore, the precision requirements could have been met with less than half the data acquired.

Nomenclature

F	ratio of selected mean square values
k	number of regressors in a model (p-1)
K	kelvin
n	number of data points used to fit a response surface model
p	number of parameters in a model, including intercept (k+1)
r	radial axis from center of fuel jet, in polar coordinates
R^2	Ratio of explained to total sum of squares
x	spanwise axis in duct
y	vertical axis in duct
z	streamwise axis in duct
σ	standard error in the regression
θ	azimuthal axis about center of fuel jet, in polar coordinates
ANOVA	analysis of variance
CARS	coherent anti-Stokes Raman spectroscopy
CIHW	confidence interval half width
df	degrees of freedom
LOF	lack of fit
MDOE	modern design of experiments
MSE	residual mean square error (unexplained variance)
PE	pure error
PIHW	prediction interval half width
RSM	Response Surface Methodology, Response Surface Modeling
SS	sum of squares
confounding	Executing an experiment so that the change in response cannot be uniquely attributed to a specific factor
$F_{critical}$	A threshold F statistic indicating minimum statistical significance

* Research Scientist, Member AIAA
** Senior Research Scientist, Member AIAA
# Associate Professor, Senior Member AIAA

level	Specific setting of an independent variable
LOF F	ratio of lack of fit to pure error components of unexplained variance
model F	ratio of model mean square to residual mean square
model mean square	variance that can be explained by model
p statistic	probability that a corresponding F statistic is not significant
parameter space, design space	Range of independent variable levels
population	a theoretical construct representing conceptually all the possible observations of a system
sample	a discrete number of observations
site:	Specific location in the design space (specific combination of independent variable levels)

Introduction

Optical measurement techniques are frequently used to study combustion, chemical reactions, plasmas, and aerospace-related flow phenomena.[1] These techniques can be characterized as either single-point or imaging techniques. Single-point techniques are generally more accurate and can provide simultaneous measurements of multiple gas properties compared to imaging techniques. Imaging techniques, on the other hand, provide spatial visualization of the flowfield, which is key to understanding important fluid mechanical and chemical processes. A common approach for mapping flowfields with high measurement precision is to translate a single-point technique's measurement volume around the flowfield of interest, assuming flow repeatability. Unfortunately, this is a time-consuming process that makes this method of testing in wind tunnels very expensive. This paper investigates a method that would optimize this strategy, allowing a substantial reduction in cost. The method is known as "Modern Design of Experiments," or MDOE. Specifically, we have used MDOE to optimize single-point coherent anti-Stokes Raman scattering (CARS) temperature measurements in a supersonic combustor.

The foundations of MDOE go back to the early part of the 20th century where formal experiment design was developed for agricultural experiments by Fisher and others.[2] Their methods allowed experiments to be designed and executed that minimize the effects of systematic errors. In the 1940s, Box and coworkers[3] developed "response surface methods" wherein an analytic model was fit to the experimental data and then tested.[3,4] This advancement allowed substantial improvements in precision compared to the state of the art at the time. Taguchi and others popularized the formal experiment design methods in the late 1970s and 1980s. Many industrial corporations adopted Taguchi's methods and some forms of his methods are still in use today. However, the aerospace instrumentation industry made very little use of formal experiment design and analysis until the mid-1990s. At that time, MDOE began to be adopted by a few researchers at NASA and elsewhere. Today the methods are gaining acceptance in the aerospace instrumentation industry. Since 1997, for example, MDOE has been used in over 40 (mainly wind tunnel) tests here at NASA Langley Research Center.[5] MDOE is used to optimize parametric studies while designing scramjet engines.[6] Lockheed Martin recently used MDOE to optimize conformal fuel tanks on an F-16.[7] NASA Langley Research Center recently began using MDOE to calibrate its model balance systems, replacing a method that had been used for several decades.[8] MDOE has been used in these wide ranging applications for a variety of reasons to be outlined in detail below. These have to do with reduced costs, improved accuracy, deeper insights into the underlying processes, and avoidance of systematic errors.

In the field of laser-based measurement techniques, great effort is expended to improve the measurement precision of a technique by a factor of two. When such advancement is made, the community at large quickly adopts it. For example, modeless dye laser designs[9,10] allowed the precision of CARS temperature measurements to be improved by about a factor of two. Now, the majority of CARS experiments being performed today (at least in the USA) use that technique. Considering the past successes of MDOE and the continued desire to improve measurement precision, we have applied MDOE to optimize the measurement of temperature in a supersonic combustor with the CARS technique. We believe that this is the first such application of MDOE to optimize a single-point laser-based measurement experiment.

Conventional Experimental Design and Execution

Before discussing MDOE in detail, conventional experimental design and execution will be reviewed briefly. Conventional laser-based measurements often begin with a loosely defined plan to "characterize a flowfield as well as possible" given the constraints (time, money, hardware limitations, etc). Measurement locations are often determined in an ad hoc manner, wherein the experimentalist attempts to "look where the interesting flow physics is." Measurements are usually taken sequentially to minimize the time required to move between set points (locations in the flow). For example, the measurement point is sequentially stepped

across the flowfield of interest. Care is often taken to obtain enough repeated measurements to produce a statistically significant mean and standard deviation of the data allowing turbulence parameters to be determined. The experiment frequently ends when either the allotted money runs out, time runs out, or the experimentalist decides (often arbitrarily) that he has acquired enough data.

The primary product of this research is usually a thesis, a conference paper, or a journal article that presents graphs, tables, probability distributions, and/or contour maps chosen to communicate the important physics of the flowfield. Uncertainty analysis is sometimes an afterthought. Other scientists wanting to obtain these data either need to contact the authors for a software copy of the data set or otherwise scan in or type in tabulated data from the paper.

Modern Design of Experiments (MDOE)

Modern design of experiments recommends a different approach on many of the issues described in the previous section. For example, a proper MDOE experiment design begins with a quantitative statement of the objective or objectives of the experiment. The objective is formulated after a great deal of consideration because the design of the experiment will depend strongly on this objective. For example, it is critical to know how the data will ultimately be used (e.g., compared with a computational fluid dynamics code). This aids in formulating specifications that can be expressed in the specific objectives and which help define quantitative exit criteria.

Once the objectives have been determined, an experiment can be designed that is optimized for achieving these specific objectives in the least time and with the lowest cost. Considerations during the design phase of the experiment include: identification of the range of the independent variables to be investigated (the parameter space), the selection of the measurement sites, and the volume of data to be acquired. See, for example, Eq. (1), which was used in this experiment to estimate data volume requirements as will be described more fully below.[§] If the cost to acquire the minimum volume of data needed to meet test objectives exceeds the budget allotted for the experiment, then one knows prior to the start of the experiment that either the resources must be increased or the objectives of the experiment must be scaled back. This knowledge alone can save considerable waste of resources. The result of the design phase of the experiment is a test matrix that describes the combinations of independent variables that will be tested.

During execution of the experiment, MDOE markedly differs from the conventional approach. In conventional experimentation, independent variable levels are typically set for convenience in some monotonically increasing order. For example, to measure the temperature distribution across a duct, the conventional approach is to start on one side of the duct and progress systematically across until the opposite side is reached. Unfortunately, this means the independent variable is changing systematically with time. It is therefore impossible to distinguish response changes that are due to the changes in independent variable from changes due to any other factor that might be changing with time. In MDOE testing, these systematic patterns are avoided. Instead, the set points determined in the design phase are executed in random order. Randomization decouples changes in independent variables from time. This enables us to distinguish the legitimate independent variable effects we seek to study from such time-varying systematic error sources as instrumentation drift, thermal effects, etc.

To illustrate the benefits of randomization, we have numerically simulated a temperature-measurement experiment. Suppose it is desired to measure the (quadratic) temperature profile across a duct. Furthermore, suppose that during the time we obtain our measurement, the temperature everywhere in the duct is increasing by 20 K between measurement points because of an undesired, uncontrollable long-term temperature drift. Using the conventional approach would produce the results shown in Fig. 1. A quadratic curve fit to the measured temperatures is shifted away

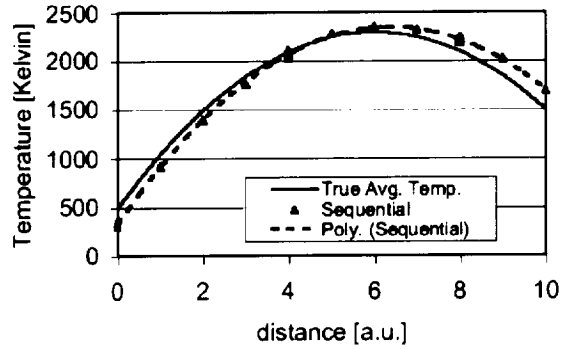

Fig. 1. Simulated temperature distribution in a duct. Measurements performed in sequential order while the temperature is increased 20 K between measurements. No random noise is superimposed.

[§] Data volume specifications vary according to the specific requirements of the experiment. The equation referenced here applies to the common situation (which applied in the current study) where a specified precision is the dominant requirement. Other variations on this formula would be used to estimate data volume requirements in other circumstances, such as when the dominant requirement is to resolve specified differences in one or more response variables.

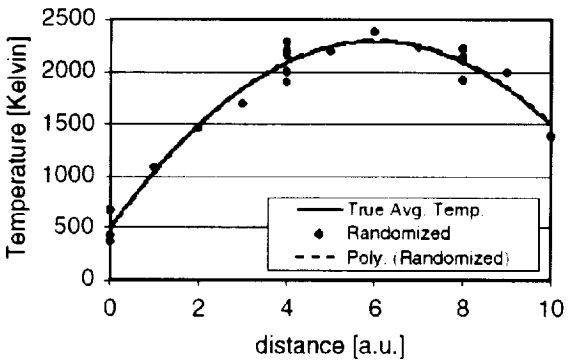

Fig. 2. Simulated temperature distribution where the order of execution of the experiment has been randomized. The temperature is increasing 20 K between measurements. No random noise is superimposed.

from the true average temperature. This is because the data on the left side of the graph falls below the true average temperature and the data on the right lies above. During execution of this experiment, the measurement location was confounded with time, which has induced a systematic error in the results.

Performing the same experiment with the same measurement locations chosen in random order yields results shown in Fig. 2. The scatter in the data is larger than in Fig. 1 because randomization has converted the systematic error into an additional component of random error. However, a quadratic curve fit through the data shows that the true average temperature was recovered, as desired. We can always acquire more data to reduce the random error if the precision requirements of the test so dictate. The important point is that randomization allows us to recover the true relationship between the independent and dependent variables, which is the raison d'être for empirical investigations. Note also the important fact that randomization defends us against all systematic errors variations, whether foreseen or not.

Replication is another important tactic that is implemented during the execution of an MDOE experiment. Replication is the process of obtaining repeated measurements at the same set point of independent variables (same x, y location, for example). True replicates cannot be obtained one after the other. Instead the set point must be changed to another value and later returned to the original measurement point to provide an opportunity for all potential sources of random error to occur, including set point error, for example.

Replication has two benefits. First, repeated measurements increase the data volume. The uncertainty in the final result decreases with the square root of the number of measurement points under commonly occurring experimental conditions. The second reason for replication is that not all of the variance in an ensemble of data can be attributed to known changes in the independent variables. After accounting for all known independent variable effects, there is always some residual *unexplained variance* that is responsible for uncertainty in the experimental results. Replication allows us to partition this unexplained variance into a component attributable to random error in the data, and another component that is attributable to analytical errors in defining the relationship between the dependent and independent variables. We call these two components of unexplained variance "pure error" and "lack of fit", and we will have considerably more to say about them below in the discussion on response surface methodology.

A third tactic that can be implemented during execution of an experiment is called blocking. Blocking involves partitioning the data set into blocks, usually differentiated by time. For example, during an experiment performed over several days, the data could be blocked by day, which would allow day-to-day variations in the experiment to be identified and accounted for. Without blocking, these day-to-day variations would appear as systematic errors.

After the experiment is completed the data is analyzed using *response surface methods* (RSM).[3-5] A response surface is an analytic model having p adjustable constants that are fit to the n measurement points, often using the method of least squares. Each proposed mathematical model is fit to the data and then evaluated with a variety of different statistical tests and other criteria. Once a model passes these tests it is a candidate for testing against data obtained during the experiment but which were withheld from the fit. The model must successfully predict the test data a statistically significant number of times to be considered a valid model representation of the data. If a linear regression model passes all these tests, then the statistical uncertainty in the mean prediction of the model, averaged over the range of independent variables, can be estimated from:

$$CIHW_{95\%} = 2\sigma(p/n)^{1/2} \qquad (1)$$

where $CIHW_{95\%}$ is the 95% confidence interval half width and σ is the fit standard error, which is independent of the model if the model is a good fit to the data. In the limit that $p = 1$, so that only the mean value of the data is determined, this formula predicts the familiar 95% confidence interval half width for the sample mean. Typically, more complicated models are used, ranging from linear ($p = 2$) to quadratic ($p = 3$) to higher order polynomials, to series expansions such as Fourier, Chebychev, and others. Note that while this equation computes a confidence interval averaged over

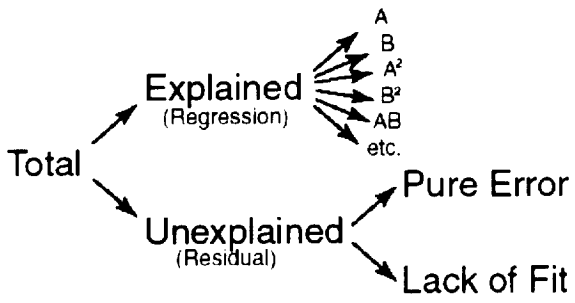

Fig. 3. Partitioning of Variance. A and B are arbitrary independent variables.

points used to fit the model, the actual confidence interval varies over the surface. The $CIHW_{95\%}$ is typically smaller near the middle of the range of independent variables and larger near the edges where there is less data.

One method used to evaluate the fit quality of potential models is known as *analysis of variance*, or ANOVA.[3,4,11] In general, variance provides a quantitative measure of the variation in a quantity. To quantify the variance the squares of the difference between each sample and some reference quantity are added (producing a "sum of squares", SS) that is divided by the number of degrees of freedom, df. The df represent the minimum points needed to uniquely quantify the sum of squares. Variance is also called "mean square error." To compute the "total variance" the reference quantity is the mean of all the samples. Alternately, one can compute the "unexplained variance" by using the model prediction as the reference quantity. Similarly, the "explained variance" can be determined by computing at each measurement location the difference between the value of the model and the mean value of the model averaged over all measurement locations and dividing by the number of degrees of freedom. In this way, the variance can be partitioned into its components, which helps quantify the quality of the fit. Partitioning of variance also helps us to interpret the model to derive a better physical understanding of the process being studied. Figure 3 summarizes the partitioning of variance and shows that the total variance can be partitioned into explained and unexplained components. The explained variance can further be partitioned into the individual model parameters. This can be useful, for example, to determine which model parameters dominate the fit, or to determine which interactions between independent variables are significant and which are not.

Partitioning the unexplained variance into "lack of fit" and "pure error" components is an important part of determining fit quality. The pure error component of the unexplained variance is determined from replicated measurements. Pure error variance quantifies the chance variation inherent in the system. An accurate estimate of the pure error is important because the part of the unexplained variance that cannot be attributed to pure error must be attributed to lack of fit. Lack of fit is the inability of the model to fit the data accurately. If the lack-of-fit component of the unexplained variance is large compared to the pure error component, the adequacy of the model is called into question.

Partitioning of variance provides several figures of merit from which the quality of the fit can be judged. The *Model F-statistic* is defined as the ratio of explained variance to the unexplained variance. This parameter provides an estimate of signal-to-noise ratio, which we would like to be a large number. A common rule of thumb for an adequate signal-to-noise ratio[3] is that the *F-statistic* should be greater than 10* $F_{critical}$, where $F_{critical}$ is tabulated in standard statistical tables for various combinations of model and residual degrees of freedom. It represents the smallest ratio of explained to unexplained variance that can be resolved with a specified level of confidence. Figure 4 shows a computation of $F_{critical}$ for a range of experimental parameters that would be expected in the present experiment. A confidence level of 95% has been assumed. $F_{critical}$ varies with the number of terms in the model but was generally less than five for the models examined in the present study. So, any fit having an *F-statistic* > 50 passed this test.

Another figure of merit is the *Lack-of-Fit (LOF) F-statistic*. This is defined as the ratio of the LOF variance to the pure-error variance. If this ratio is near unity then there is unlikely to be significant lack of fit. In other words, statistically, it is a good fit. An associated statistic is called the *LOF p-statistic*, which describes the probability that the measured *LOF F-statistic* could be as large as it is due just to random error. A small *LOF p-statistic* (less than 0.05 by one common convention) argues against a good fit.

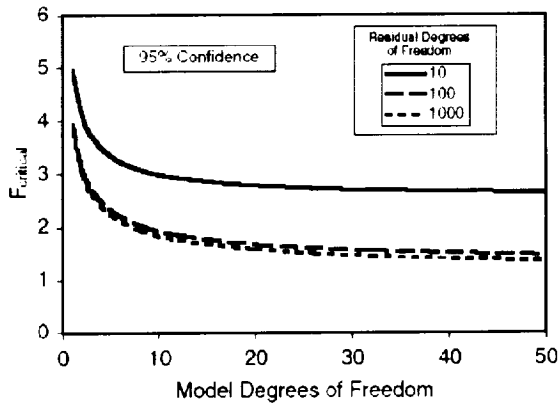

Fig. 4. Computation of $F_{critical}$ for the *F-statistic* test.

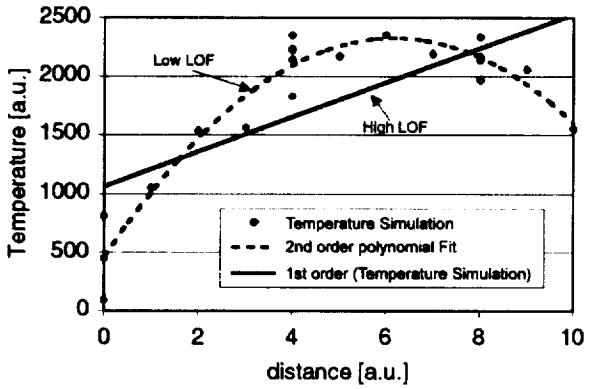

Fig. 5. Simulated temperature data to illustrate the concept of lack of fit. Random noise with a standard deviation of 100 K of has been added to the same "true average temperature" shown in Fig. 1.

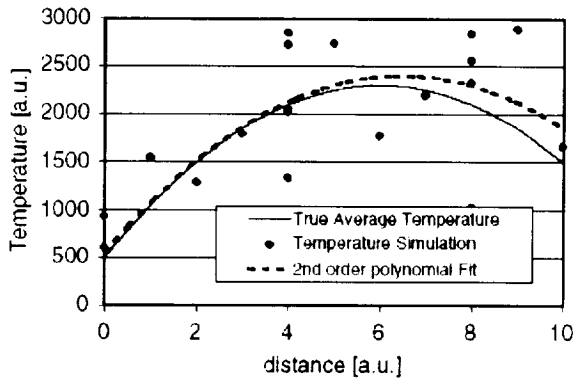

Fig. 6. Simulated temperature data to show failure of the *Model F-statistic* test. Random noise with a standard deviation of 500 K of has been added to the same "true average temperature" shown in Fig. 1.

Figures 5 and 6 illustrate the concepts of lack of fit and signal-to-noise ratio (*Model F-statistic* test). Figure 5 shows two models that have been fit to a set of simulated experimental data that includes random noise. Though the first-order model represents a best least squares fit to the data, it shows significant deviation from the data at most locations. In particular, the deviation between the first-order model and the data is much larger than the scatter in the data, so the *LOF F-statistic* would be large for this fit. The second-order model, on the other hand, fits the data very well. More of the difference between the model and the data is due to chance variation in the data than to lack of fit, so the *LOF F-statistic* would be relatively small.

Figure 6 shows an example where the scatter in the data is much larger (500 K standard deviation). In this case the *Model F-statistic* is not large enough to exceed our criterion of $10*F_{critical}$ and the model fails the lack-of-fit test. The large scatter would be revealed by the pure-error component of the unexplained variance, and would suggest that more data might improve the fit. If the pure error were small, we would have to attribute the lack of fit to an inadequate model, and would therefore have to fit a more elaborate model – typically one with higher-order terms.

Another figure of merit is R^2. This is the ratio of the explained sum of squares to the total sum of squares (where the sum of squares is equal to the variance times the number of degrees of freedom). R^2 provides an estimate of the fraction of the variance that is explained by the model. For example, if $R^2 = 0.8$, then the model is said to explain about 80% of the variance present in the data.

Graphs of residuals also provide information about fit quality. Residuals are the difference between sample measurements and the model prediction. Residuals should not show any trends when graphed against any of the independent variables, the model predictions, or time. If substantial trends are observed in residuals then the model probably does not represent the data adequately. Large residuals ("outliers") should be carefully examined, but should not be deleted without justification. All information provided by the data about the quality of the fit is carried in the residuals, and while an outlier may signify a "bad" data point, it may also identify an important deficiency in the model.

If the model passes all the above tests, one needs to determine whether the uncertainty, specified for example by Eq. (1), meets the test requirements. If the requirements are not met, then it is possible that another model could be found that would fit the data better, resulting in an acceptably low level of uncertainty. (Note that this implies an a-priori definition of "acceptable," which is a standard requirement in MDOE testing.) A better model can often be found by transforming either the dependent variable or one or more of the independent variables. This can improve fit quality or reduce the number of parameters in the model, thereby reducing the uncertainty.

If the model meets the precision requirements then it is a candidate for testing against data withheld from the fitting process. Typically, ~5% of the data is withheld to assess model adequacy. The model must successfully predict the temperature in a statistically significant fraction of trials for the model to be accepted. The model is said to successfully predict the value of a measured data point if that point agrees with the model prediction within the model prediction interval. For a model with negligible lack of fit, the 95% prediction interval half width, $PIHW_{95\%}$, is approximately equal to 2σ where σ is the standard error in the fit. For example, suppose $\sigma = 100$ K and the model prediction at a given site is 1000 K. There is no more than a 5% probability that a confirmation point would fall outside the range of 800 K and 1200 K due to ordinary chance variations. However, just as we

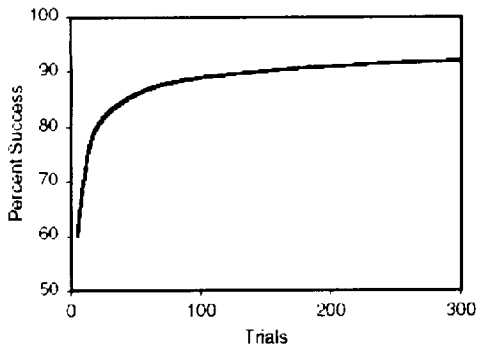

Fig. 7 The minimum percentage of trials expected to be successfully predicted if there is at least a 99% probability that the number of successful confirmations is consistent with the 95% prediction interval of an adequate model.

would not require 100 tosses of a coin to produce exactly 50 heads in order to declare the coin fair, neither do we require exactly 95% of all confirmation points to fall within the 95% prediction interval. (Surely 94 successes out of 100 trials would not invalidate the model, just as it is not unlikely that 96 points might fall within the 95% prediction interval half-width in any one set of 100 confirmation trials.) Just as it happens that 99% of the time, a fair coin will produce between 37 and 63 heads in 100 trials, so it is that there is a 99% probability that in 100 trials, 89 or more confirmation points (not 95!) will fall within the 95% prediction interval of an adequate model. For a lower number of trials, say 10 trials, only seven or more successes are required. Figure 7 reveals the minimum percentage of successful confirmations required of a model for there to be at least a 99% probability that this percentage is consistent with the 95% prediction interval of an adequate model. This percentage is graphed in Fig. 7 versus the number of trials.

The payoff for doing all this extra work – designing the experiment, acquiring the data in random order, and then analyzing the data with RSM – can be profound. First, there is usually a substantial improvement in accuracy, particularly, avoidance of systematic error because of randomization. Second, the entire data set can be compactly represented by an equation and a handful of constants that can be used by the customer to compute the dependent variables anywhere in the parameter space. Third, and most important, there is a marked improvement in precision compared to conventional methods because of using response-surface methodology.

To illustrate the improvement in precision possible with MDOE, Fig. 8 compares MDOE to a conventional experiment where replication has been used in both experiments to improve measurement precision. All of the curves assume the same number of data points (1000) and same standard deviation in the data (100 K). Note that for measurements with errors that are normally distributed about a mean of zero, the 95% confidence interval half-width of an n-point sample is approximately $2\sigma/(n^{1/2})$. The corresponding value for a fitted surface varies over the surface, but its average value scales as $p^{1/2}$. See Eq. (1). For a small number of measurement locations (for example, three), the conventional single-point method provides comparable uncertainty to an MDOE response surface fit having three parameters. In this case, the 1000 points are spread equally among three sites and the 95% confidence interval half width in both cases is ~10 K.

Suppose, however, that the flow may have a substantial amount of spatial structure that one would like to map. If the number of measurement points is increased, the number of measurements per location decreases accordingly. Consequently, the uncertainty estimated from data acquired at only one location will have a corresponding increase in measurement uncertainty. On the other hand, the MDOE method maintains a constant measurement uncertainty, assuming that the same three-parameter model is used. If a higher order model is used to fit a more complicated flow structure, the simulation shows that MDOE still provides a marked increase in precision compared to the conventional single-point statistics method. For the case of a 10-parameter model used to fit data obtained over 100 independent spatial locations there is more than a factor of three improvement in measurement uncertainty. Alternately, MDOE could obtain the same measurement uncertainty as the conventional method with nearly 1/10th the number of data points! That amounts to a substantial cost savings.

In this paper, we use the term "costs savings" loosely to mean reduction in the number of

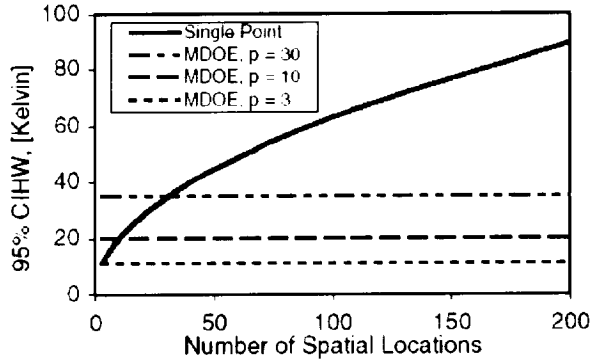

Fig. 8 Comparison of measurement uncertainty (95% confidence interval half widths) between MDOE and conventional single-point statistics as a function of the number of spatial locations probed. The total volume of data is held constant at 1000 points. A 100 K standard deviation is assumed.

measurement points required. The real costs of doing experiments can be computed many different ways, and often involve a large initial investment to build the facility, for example. A comprehensive analysis of all such costs is beyond the scope of this paper. Additionally, it is important to note that randomization and replication usually reduce the rate of acquisition of data, offsetting some of the reduction in costs. However, in many prior applications of MDOE, substantial cost savings have been achieved.[5]

One might question how simply fitting a curve through the data would increase its precision. It appears too good to be true. The key point is that by fitting a curve through the data, information is shared from neighboring spatial locations. Suppose you have obtained temperature measurements at five locations along a line where the temperature is slowly increasing. If another measurement is desired between two of the existing points, it would not take many measurements to establish whether the new location agrees with the trend established by the other points. Information is shared and fewer measurements are required to achieve the same uncertainty. Using the single point method, the experimentalist starts "from scratch" at each new spatial location and many measurements are required to reduce the uncertainty in the mean.

Considerations for Mapping Temperature in a Supersonic Combustor

The description above outlines the way an ideal experiment would be designed, executed, and analyzed using MDOE. Unfortunately, some compromises that prevented the full implementation of MDOE were required in the present experiment. In this section, we briefly describe the experimental setup as it relates to the current paper and then discuss how MDOE was implemented.

Experiments were performed in NASA Langley Research Center's Direct-Connect Supersonic Combustion Test Facility (DCSCTF), which is a vitiated, blowdown wind tunnel. The supersonic combustor model consisted of a short rectangular duct containing a rearward-facing step, after which gaseous hydrogen fuel was injected. The supersonic combustor operated with a steady flow time of 10-20 seconds.

We used planar BoxCARS to make single-shot broadband nitrogen CARS temperature measurements in the combustor.[12] During the flow time, 100-200 single-shot temperature measurements were obtained. CARS spectra, acquired from an intensified CCD linear array attached to a spectrometer, were fit with a library of theoretical curves for a range of temperatures and N_2 concentrations to determine the gas temperature on each pulse of the laser. Thus, a database of x, y, z locations, temperatures, and N_2 concentrations was generated for five measurement planes in the flowfield for unpiloted operation and three planes when H_2 pilot fuel was injected upstream of the main fuel injection. A series of measurement in a stable Hencken flat-flame burner determined that the precision of the CARS measurement technique was ±6% of the measured temperature (standard deviation of 3%). The flame measurements reported in Ref. 12 showed that the CARS system produced temperatures that were systematically high compared to calculated values by ~150 K in the rich region of a hydrogen/air flame. Good agreement was found for stoichiometric and lean flames. However, this experiment was recently repeated and this systematic error was not observed. The mean measured temperatures agreed with computed values to within 70 K on average over a range of stoichiometries from 0.5 to 4.0 and no systematic bias in the measured temperatures was observed.[13] The systematic bias observed in Ref. 12 is thought to be caused by spatial nonuniformities present in the flame, though this point is still under investigation.

Figure 9 shows the resulting temperature maps obtained in the supersonic combustor.[12] Briefly summarizing the results, the vitiated air flow enters the test section at about 1160 K. For the unpiloted case, cold fuel, with a stagnation temperature of about 300 K, is injected between planes 1 and 3. Evidence of a small amount of combustion occurs around the periphery of the fuel jet in plane 3 where the temperature exceeds the incoming freestream value. The temperature of the cold jet increases between planes 3 and 5, but most of the combustion occurs between planes 5 and 6. Planes 6 and 7 show hot combustion products on the top and bottom of the duct and remnants of the cold fuel jet near the middle of the duct.

The current paper describes in greater detail how MDOE was applied to this experiment and how the analytic surfaces were fit to the data, to produce the temperature maps shown in Fig. 9. The analysis in this paper is limited to plane 3, unpiloted operation, which was thought to be the most challenging measurement plane to analyze due to the large temperature gradients present.

The objectives for the present experiment were determined from interviews with the customer, a computational fluid dynamics expert who has subsequently computed the flow.[14] Together it was decided that the goal of the present experiment would be to map the flowfield with a specified precision, in as many planes in the combustor duct as resources would permit. From discussions with the CFD expert, we established ±50 K as the required 95% confidence interval for model predictions. For resource planning purposes, we computed the volume of data necessary to produce a model with such a 95% confidence interval,

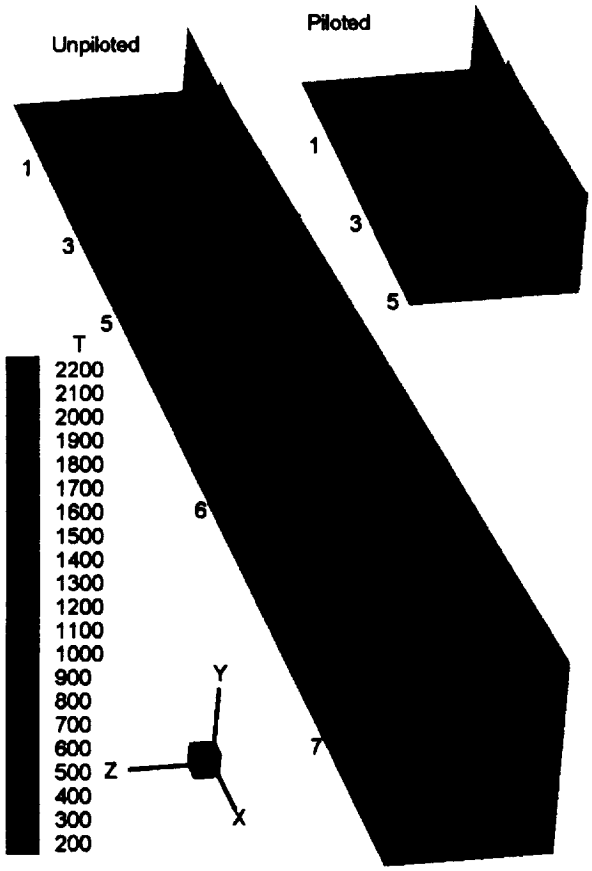

Fig. 9. CARS temperature maps in the combustor duct. See Ref. 10 for details.

averaged over all the points used to fit the model. Also, from prior measurements in the same facility[15] we knew that turbulent fluctuations in the flow had a standard deviation of about 300 K. Furthermore, observing the spatial distributions in past measurements, we determined that we would probably fit the data with response surface having approximately 20 parameters. Using Eq. (1) the required number of data points was estimated to be 2880 per measurement plane.

If we had instead used the conventional approach of acquiring many temperature measurements at a single location to reduce uncertainty in the mean, and if we targeted the same precision requirements, 144 temperature measurements would have been required at each site. The MDOE budget of 2880 points per plane then corresponds to only 20 measurement locations if the conventional method had been used. These would perhaps be enough spatial locations to measure the temperature along two or three lines in the flowfield. But, for the same cost, MDOE allows us to map the temperature over the entire plane.

The data acquisition rate was 10 Hz and the tunnel typically operated for 10-20 seconds per run, so that ~100-200 shots could be acquired per run. Thus a minimum of 20 runs would be required per measurement plane to meet the precision requirements. Because the tunnel must be allowed to cool down between runs, we were limited to four or five runs per hour. The CARS apparatus and the DCSCTF require about an hour each of set-up and takedown time. So, an entire day was just enough time to map the temperature in a single plane with the required measurement precision. We obtained between 2000 and 4000 instantaneous temperature measurements per plane.

Given a data rate of one plane per day, our budget limited the number of measurement planes we could acquire. Budget constraints included real dollar costs for facility time, cost for the H_2 gas, as well as availability of staff to run the tunnel, run the CARS system, and ensure the safety of the workers and facility. The stated objective then was "to map the mean temperature in five or more planes of the supersonic combustor with a measurement precision of better than ±50 K with 95% confidence." In the end, seven measurement planes were acquired over 10 days of operation. This occurred over about two months of calendar time.

The next aspect of the experiment design to be considered was site selection. Ideally, we would have selected sites according to the D-optimal design,[16] which has several features that make it a desirable measurement pattern. Among other benefits, the 29-point D-optimal design, shown in Fig. 10, has symmetry properties that maximize the accuracy of fit coefficients used in response surface methodology. Ideally, the CARS measurement volume would be translated to one of these locations and a single temperature measurement would be obtained. Then the measurement volume would be translated to one of the other sites, chosen at random, where a second temperature measurement would be obtained, and so on. Each location would be revisited many times, providing the number of replicates indicated at the locations in the figure.

Unfortunately, in the present experiment the typical time required to translate between points in the measurement volume is about 20 times longer than the 0.1 seconds between measurements. This data rate of 10 Hz is set by the repetition rate of the laser. If we were to use the full randomization preferred by MDOE, our data rate would be cut by a factor of 20, which would have prevented us from achieving our precision goals without exceeding our resource budget.

A compromise solution was found that implemented as much randomization as possible. Two types of measurements could be performed at the maximum data rate. One type of measurement was obtained by scanning the probe volume horizontally or vertically through the flowfield using a system of periscopes driven by stepper motors. A second type was performed at fixed locations in the duct for the

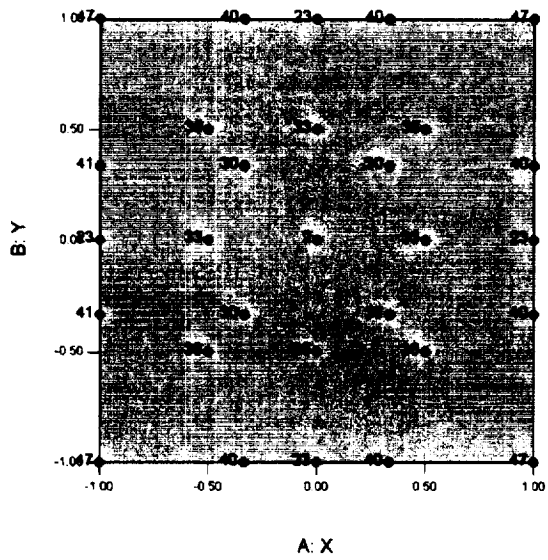

Fig. 10. D-optimal design for determining optimal locations for spatial measurements.

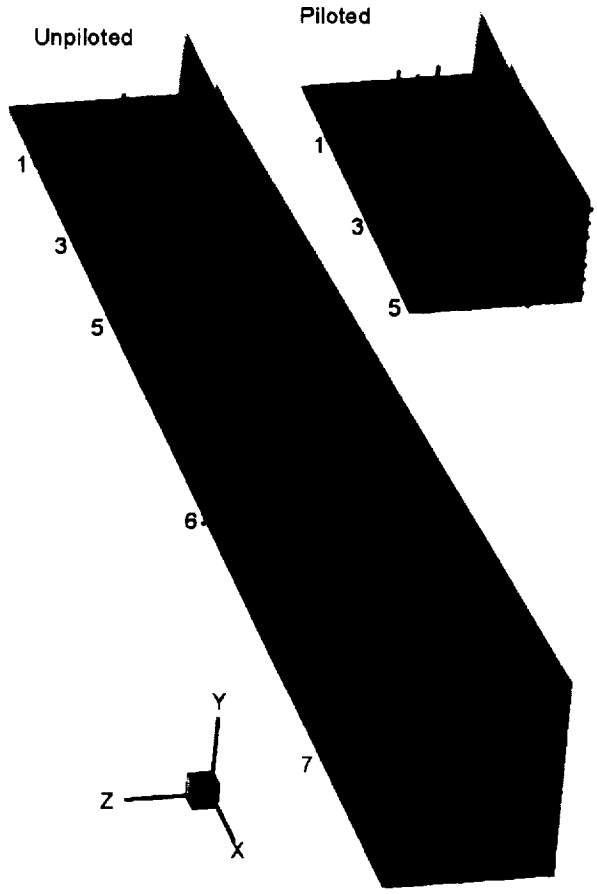

Fig. 11. Site selection for the experiment.

entire duration of the run. The fixed location measurement scheme potentially could have been applied in a D-optimal site selection. However, performing the entire design would have required 29 runs that would have produced far more data than required for the precision requirements. We believed that decreasing the number of set points by a factor of two, to match the precision requirements, would have sampled the flowfield too sparsely. So, a hybrid method was adopted where both types of measurements – fixed and scanned – were used. Thus, the D-optimal design was abandoned in favor of a rectangular grid. This was supplemented by six to eight fixed position measurements, depending on the measurement plane. All fixed locations were distributed uniformly in the vertical direction on the spanwise center of the flow. We alternated randomly between fixed and scanned runs. We also randomized the directions of the scanned measurements (up/down or across/back). Figure 11 shows the sites selected for the different measurement planes in the experiment. For completeness, it should be mentioned that blocking was not invoked in the present experiment because no block effects were identified.

After the experiment was performed, temperatures were computed from the raw CARS spectra. See Ref. 12 for details of this procedure. The x, y locations of the measurement volume and the corresponding temperatures from all runs in a given plane were written to data files, one line for each individual temperature measurement.

Two different statistical analysis programs were used to fit the data: Design-Expert®[16] and TableCurve®3D.[17] These programs have many common features, including automatic fitting of surfaces to data and automatic computation of the statistical figures of merit (*Model F-statistic*, R^2, etc). TableCurve®, however, does not allow model terms to be removed as easily as Design-Expert®. Removing model terms is very important in the present application because reducing the number of terms p increases measurement precision, according to Eq. (1). It is often found that more than half of the terms in the models are insignificant. So, by removing these terms one can gain an increase in precision of a factor of about 1.4. Unfortunately, the only candidate model functions in Design-Expert® are polynomials, whereas TableCurve® provides thousands of different model forms, including Chebychev, Fourier, Sine and Cosine Series, etc. Thus, both software packages were used in the analysis.

Nine different proposed models were evaluated prior to settling on the best one. For ease of explanation, these will be described in order of increasing complexity, rather than the order in which they were performed. Six different proposed models were fit to the entire data plane using Cartesian coordinates: 3rd-, 4th-, 5th-, and 6th-order polynomials

and two different versions of the Cosine Series Bivariate Order 6 Function. One proposed model partitioned the measurement plane into four subregions and used lower order polynomial models in each region. A transformation from rectangular to polar spatial coordinates was used for the other two proposed models, which were fit with 3rd-order polynomials in r and θ. One of these polar coordinate analyses involved transforming the dependent variable.

During the analysis of the data, three extreme residuals were removed out of a total of 2829 measurements. There were perhaps 50 smaller residuals that were nonetheless candidate outliers, but these were retained because we could not say with high confidence that these were likely to be the result of spurious measurements.

Results

Polynomial Fits to Entire Cartesian Surface

Equation (1) shows that the lower the order of the model (the smaller the p) the better. So the first proposed model was a 3rd-order polynomial in the two independent variables, x and y:

$$T = a + bx + cy + dx^2 + exy + fy^2 + gx^3 + hx^2y + ixy^2 + jy^3 \quad (2)$$

This equation has 10 free parameters p. Note that it contains cross terms (e.g., xy, x^2y, and xy^2) whose magnitude describes the interactions between the independent variables. Fitting Eq. (2) to the temperature measurements from plane 3 yielded unsatisfactory results. Four of the model terms were insignificant and were removed. While the overall model passed the F test indicating reasonable signal to noise, it did not pass the lack of fit tests. Visually comparing residuals showed several systematic trends, confirming a poor fit. Furthermore, the temperature surface looked unrealistic (concave up).

The order of the fitting polynomial was increased sequentially to 4th-, 5th-, and 6th-order. Each time, the model F test passed and the fit improved. These trends are illustrated in Fig. 12. Notice that the standard error in the fit, σ, decreases with increasing order number: more terms allow the model greater flexibility to explain trends in the data. Also note the increase in the computed $CIHW_{95\%}$. This trend is caused by the increase in p as the model order increases. From (1) it is apparent that $p^{1/2}$ is growing faster than σ is decreasing. Recall that the computed $CIHW_{95\%}$ is only valid if the model fits the data (which none of these do). The 6th-order model, which has 18 significant terms, is the only one of these models that passes its statistical lack of fit test. The 6th-order polynomial temperature map is shown in Fig. 13(a). Upon close inspection of the model predictions and the residuals, important systematic discrepancies between the data and the fit were discovered. The worst problem occurred at the center of the cold fuel jet where the model predicted ~350 K whereas the gas temperature measured with CARS was ~250 K. Clearly there is some localized lack of fit. It is worth noting that we suspect lack of fit in the model even though it passed the statistical lack of fit tests. This is probably because there is comparatively little data in the fuel jet.

The overwhelming majority of the measurement plane is fit satisfactorily, and a small (but important) part is not. This is an example of why possessing subject knowledge is very important for performing data analysis, and particularly for model fitting.

For comparison with CFD, accurate modeling of the fuel jet is critical. For this reason, this 6th-order polynomial fit was deemed unsatisfactory. The next logical step would have been to use a 7th-order polynomial model. Unfortunately, the software did not allow higher than 6th-order polynomial models. So, another method for improving the fit needed to be found. The ANOVA figures of merit for the 6th-order polynomial and the rest of the fits discussed in the paper are summarized in Table 1.

Polynomial Fits to Sub-Zones

A method that is commonly used in fitting complex surfaces is to break the surface up into smaller subspaces. Each subspace can then be fit with a lower-order model, each having fewer parameters, potentially resulting in improved fits and reduced $CIHW_{95\%}$. We use this approach and partitioned the measurement planes into four sub-regions, or zones, as illustrated in Fig. 14. Zones 1 and 3 were adequately fit by 3rd-order polynomials. Zone 4, which contains the fuel jet, required a 4th-order polynomial fit, which did a very

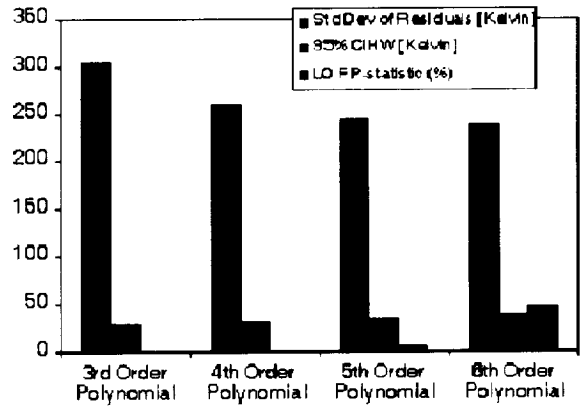

Fig. 12. Trends in σ, $CIHW_{95\%}$ and *LOF p-statistic* with increasing polynomial order of model.

satisfactory job of fitting the fuel plume. Zone 2 provided an interesting result: this region had very little curvature compared to the chance variations in the data. The overall model F test failed on all polynomial models attempted in this region. This indicates that there is no significant trend in the data with x or y, compared to the variability in the data. In this case, the entire sub-region is best modeled by the mean of the data in that region.

In order to compare the quality of this fit to the others reported in the paper, an approximate $CIHW_{95\%}$ was computed by weighting the $CIHW_{95\%}$ values for the individual regions by the number of points in each region and dividing by the total number of points fitted. Table 1 shows that the method fails to reduce the $CIHW_{95\%}$ compared to the 6th-order polynomial. However, it is a better fit than the 6th-order polynomial because it more accurately captures the most important features of the flowfield. Figure 13(b) shows the resulting temperature map. One drawback of partitioning into sub-zones is evident from the temperature map: discontinuities in temperature exist at the borders of the zones. This is unaesthetic, but not unscientific. The model actually predicts that a given sample would occur between this surface mean and the $\pm PIHW_{95\%}$. This is illustrated in Fig. 15 where a horizontal slice through the measurement plane is compared with the model. This slice crosses zones 1, 4, and 3, in that order. The correct interpretation of this figure is that the model predicts with 95% confidence that seven out of 10 new measurements (as described by Fig. 7) would fall between the dashed lines in the figure.

Model	*p*	*Fstat*	*PIHW*	*CIHW*	R^2
6th order polynomial	18	230	477	37	0.59
Polynomial fits to four partitioned zones	<14	-	-	38	-
Cosine Series Bivariate Order 6, #1	28	185	450	45	0.64
Cosine Series Bivariate Order 6, #2	13	425	447	30	0.64
Polar coordinate transformation	6	898	471	22	0.61
Polar coordinate and ln(T) transformation	6	1038	479	22	0.64

Table 1. Summary of fit results for select models. *PIHW* and *CIHW* are based on 95% confidence. All models represented in this table pass the *LOF F-statistic* and *P-statistic* tests, except where noted in the text.

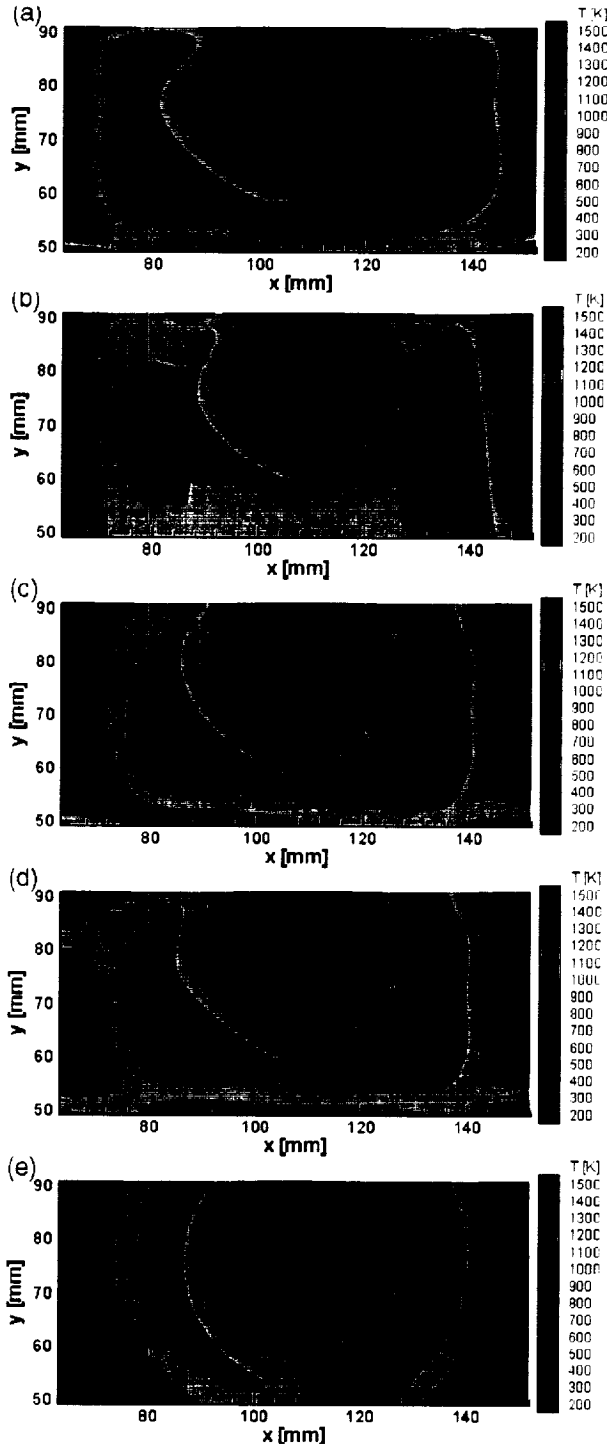

Fig. 13. Temperature maps resulting from fitting different proposed models. (a) 6th-order polynomial, (b) polynomial fits to four sub-regions, (c) 27 term cosine series bivariate order 6 function, (d) 12 term cosine series bivariate order 6 function, (e) polar coordinate transformed data fit with 3rd order polynomial

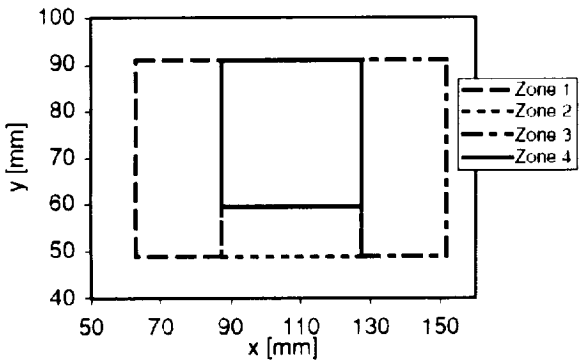

Fig. 14. Partitioning of measurement plane into four sub-zones.

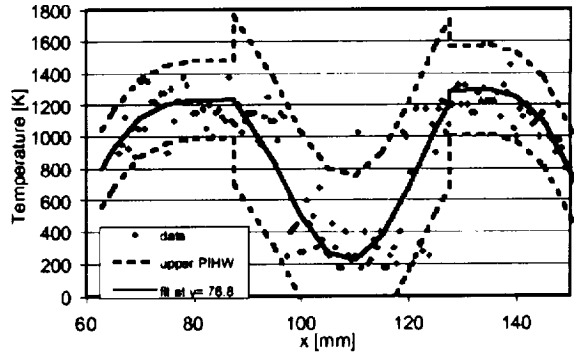

Fig. 15. Comparison between model prediction (four-zone polynomial model) and single-shot temperatures for spanwise cut through the flow at y = 76.8 mm.

Cosine Series Bivariate Model

In an attempt to model the temperature distribution with a more suitable basis function than polynomials, the TableCurve® program was used to find a suitable model. A promising model was the Cosine Series Bivariate Order 6 function. This function was chosen because it offered a compromise of a very good fit to the data (based on *Model F-statistic*, lack of fit *F*- and *P-statistics*, R^2, and standard error in the fit, σ) while having fewer parameters than many of the other functions. This function is similar to the first few terms of a Fourier series but contains only cosine functions and has products of cosines as well as the usual cos(x), cos(2x), cos(3x), etc., terms. The full 6th-order model has 28 parameters. The fit produced by TableCurve® is shown in Fig. 13(c).

The ANOVA results for this model suggested that more than half of the model parameters were insignificant. Removing these terms would decrease the $PIHW_{95\%}$ substantially. So, a data file was created that would allow Design-Expert® to implement this fit. This was achieved by creating a spreadsheet that contained a column for each of the 27 terms in the model. The functional shape of each term (e.g., cos(3x)) was then computed in each column. When the spreadsheet was read into Design-Expert®, a model that was first-order in each of 27 different independent variables was fit to the data. As expected, after insignificant terms were removed, only 12 terms plus intercept remained, so that p = 13. The resulting temperature map is shown in Fig. 13(d). The fit is similar to Fig. 13(c). However, because p has been reduced from 28 to 13, the accuracy to which each of the coefficients in the model has been determined is substantially higher. With fewer model parameters, there is more data per parameter from which to determine the values of the parameters. As shown in Table 1, the resulting precision is markedly improved: from ±45 K to ±30 K. Figure 16 shows the residuals plotted against the spanwise direction, x. The residuals show no significant trends versus x except at the extremes, confirming that the fit over most of the surface is good.

Figure 17 compares model predictions and prediction intervals to the experimental data. The model fits the general trends of the data very well. However, the model does not capture every subtlety of the data. Higher order terms would be required to fit sharp discontinuities in the data. Such higher order models would require more parameters and would yield a higher $PIHW_{95\%}$.

Variable Transformation: Polar Coordinates

In an effort to reduce the parameter count even further, we attempted to take advantage of the near-radial symmetry of the fuel jet. We transformed the x, y coordinates into radial coordinates: r, θ, where $r^2 = (x-x_0)^2 + (y-y_0)^2$ and $\theta = \tan^{-1}((y-y_0)/(x-x_0))$ where care was taken to add 180 degrees to θ when $x < x_0$. Figure 18 shows the result of the transformation. The center of the coordinate system was chosen to be at the center of the fuel jet (x_0 = 108.6 mm, y_0 = 76.1 mm). Such a

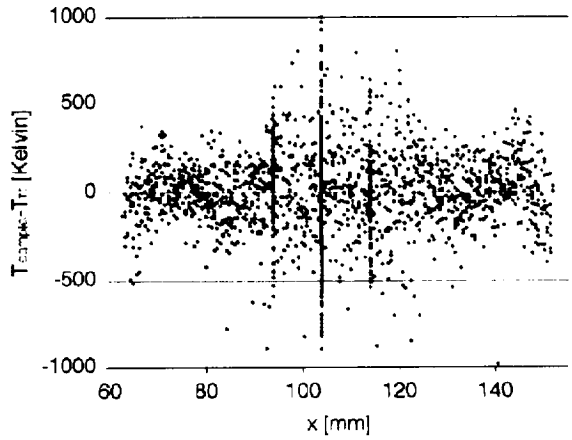

Fig. 16. Residuals plotted versus x.

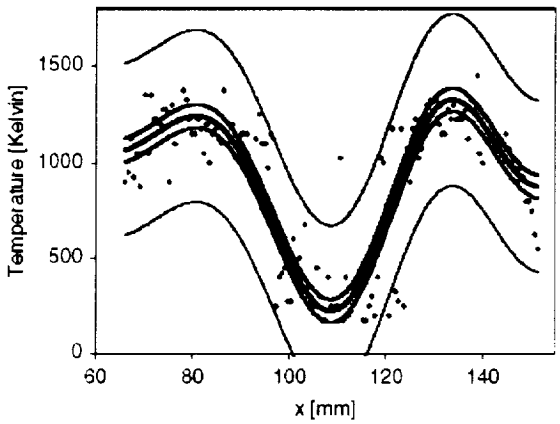

Fig. 17. Comparison between model predictions and single shot temperatures for Cosine Series Bivariate Order 6 model #2. This is a spanwise cut through the flow at $y = 76.8$ mm. The thick solid line in the middle is the model prediction. The two thinner lines above and below the model prediction are the 95% confidence interval half widths. The thin lines furthest from the model prediction are the 95% prediction interval half widths.

transformation greatly simplifies the functional form required to fit the data. For example, a temperature profile in the shape of an inverted cone would be very difficult to fit in Cartesian coordinates; it would require many high-order terms. But, in polar coordinates, an inverted cone maps to a planar surface that can be fit by the simple model, $T = a - br$. This variable transformation worked as advertised; the fit order could be reduced substantially – to 3rd-order – and the number of parameters could be reduced to six. This resulted in a low $CIHW_{95\%}$ as shown in Table 1. Unfortunately, there were several undesirable consequences of this method. First, the model temperature trends towards a large negative temperature at small r, which is unphysical. The polynomial should be forced to have zero slope at $r = 0$. Similarly, when the data is fit in polar coordinates, it would be desired to have a periodic boundary condition in θ.

A natural logarithmic transformation in the dependent variable (temperature) was found to correct the first problem. Fitting ln(T) instead of T forces the model to be better behaved at small r. This transformation also causes a significant improvement in the fit, as evidenced by the increase in R^2 in Table 1. Furthermore, it compares much better with the data in the fuel jet. The resulting temperature map is shown in Fig. 13(e). Comparing this map with the others in Fig. 13 reveals that an artificial symmetry has been imposed on the data by the polar coordinate transformation. Perhaps this is caused by not retaining high enough order terms. However, we regard with suspicion the visible circular patterns, particularly the corkscrew

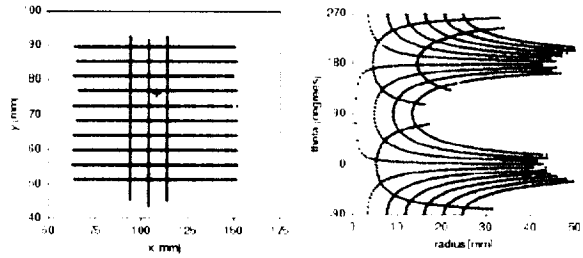

Fig. 18. Rectangular to polar coordinate transformation. The red crosshair marks x_0, y_0.

shaped variation in temperature. The residuals provide further evidence of an unsuccessful fit. The residuals plotted against θ show no significant trends, but the residuals plotted against radius, shown in Fig. 19, display some weak but significant trends. Even though this model passes all the statistical tests and has the smallest $CIHW_{95\%}$, we believe that this model does not adequately represent the data.

Discussion

The various methods of fitting the data have their relative merits. While the 6th-order polynomial fit was easy to perform, it produced a temperature map that disagreed with the experimental data in a critical region of the flowfield: the cold fuel jet. Partitioning the surface into four smaller surfaces allowed lower order polynomials to accurately fit the experimental data, but this process was very time consuming and it produced the second worst $CIHW_{95\%}$ values of all the fits shown in Table 1. The Cosine Series Bivariate Order 6 function fit the surface well with a minimum of effort. However, the large number of model parameters caused the fit uncertainty to be the worst in Table 1. This problem was corrected by removing the insignificant

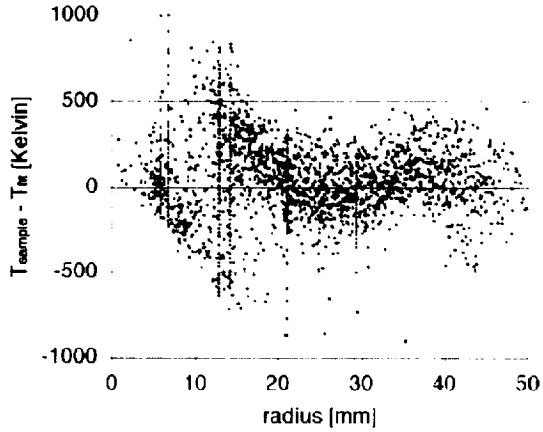

Fig. 19. Residuals plotted versus radius, r.

terms in a subsequent analysis, producing a $CIHW_{95\%}$ equal to ±30 K. Inspection of residuals shows no substantial trends. The polar coordinate transformation of the independent variables, combined with the natural logarithmic transformation of the dependent variable produced a result that had excellent statistical properties, but imposed an artificial symmetry on the flowfield. Also this model shows some small but substantial trends when residuals are plotted against radius. We conclude that the model that most accurately represents the measured temperatures is the cosine series bivariate function with insignificant terms removed.

After passing these various criteria, the model is considered to be a "candidate model" for validation. The model was tested against a portion of the original data selected at random that had been set aside and not included in fitting the model (5%, or 140 points). According to Fig. 7, to validate the model, it must predict >90% of the trials correctly, or at least 126 out of the 140 trials. In fact, the model predicted 128 out of 140 correctly (or 91%), so it was said to have passed the confirmation test.

It is useful to compute whether the MDOE method did in fact reduce the volume of total data acquired in the experiment, as predicted by Fig. 8. In a similar experiment previously conducted in the same facility, Smith et al.[15] mapped the temperature in a different supersonic combustor. They determined the mean temperature in the conventional way by taking ~70 replicates at each of 63 points of a 9 by 7 grid. If they had had the same standard deviation (σ = 223 K) as in the present experiment, they would have obtained 95% confidence level uncertainties in the mean values of temperature at each of those points of ±53 K. To further reduce their uncertainty to the ±30 K level obtained using MDOE would have required a total of 225 measurements per location, or ~14,000 points compared to the current experiment in which ~2800 points were obtained. MDOE allowed us to get the same uncertainty with a factor of five fewer points - a substantial reduction.

In the current experiment, we could have reduced the data volume by a factor of $(50/30)^2$ or ~2.5 and still met the precision requirements of ±50 K at 95% confidence. However, the opposite could also have been true: If the turbulence level had been twice what was anticipated prior to the experiment, we would have failed to meet our precision requirement. So the amount of data obtained in the current experiment was probably appropriate. It was ample to protect us against incorrect assumptions of the nature of the flow, yet it was not so great as to have incurred substantially more time and expense than needed to satisfy the quality objectives of the experiment. However, there is another, better, solution to the resource scaling problem. If the CARS spectra could be analyzed as they were being acquired, or in between tunnel runs, then a surface fit could be performed as the experiment progressed. The fit uncertainty would be constantly monitored. Once the precision requirements were met, the experiment could be terminated, having acquired the right amount of data. This approach would prevent acquiring too much data. The costs saved could then be used, for example, to study other measurement planes, fuel flowrates, model configurations, etc.

In addition to the substantial cost savings, MDOE defended against systematic errors through randomization. In fact, we did see some trends in the residuals when plotted against time, a tell-tale sign that the kind of systematic variation against which randomization is intended to defend was in fact present during the experiment. During certain runs, for example, the gas temperature appeared to be systematically increasing with time. These trends need to be analyzed more closely. Nonetheless, randomizing the order that the data were obtained allowed us to defend against such bias errors.

Another benefit of the response surface methods incorporated in MDOE is that the data can be compactly presented. This facilitates comparison between the data and theoretical or computational predictions of the flow, which is frequently an end use for data obtained using laser-based measurement techniques. For example, the surface fit for the 13-parameter Cosine Series Bivariate Order 6 model is shown in Eq. (3):

$$
\begin{aligned}
&\text{Temperature} = \\
&1068.2 + \\
&103.2\cos(Y') + \\
&117.3\cos(2X') + \\
&-91.9\cos(3Y') + \\
&-180.8\cos(4X') + \\
&36.5\cos(5X') \\
&25.2\cos(5Y') + \\
&-45.7\cos(X')\cos(Y') + \\
&-109.6\cos(2X')\cos(Y') + \\
&143.2\cos(4X')\cos(Y') + \\
&191.2\cos(2X')\cos(3Y') + \\
&-48.2\cos(5X')\cos(Y') + \\
&139.5\cos(4X')\cos(2Y').
\end{aligned}
\tag{3}
$$

Unfortunately there are certain cultural barriers that are likely to retard the rate at which the laser-based measurements community adopts MDOE. The primary obstacle is the haste with which many scientists in this field tend to approach experiments. MDOE involves carefully planning an experiment, which can be time consuming. However, the time spent in designing a good experiment is negligible compared to the time spent trying to make sense out of a poorly planned one.

But designing an experiment with MDOE seems time consuming compared to the conventional method, in which the final design of the experiment often occurs moments before it is executed. Another barrier to usefully applying this method is that the user must learn about certain statistical methods (e.g., ANOVA) that might presently be unfamiliar. Still another barrier is the time required to analyze the data, which can frustrate the natural human tendency to demand a final result immediately upon completion of the experiment. Nonetheless, we believe that MDOE will gain increasing acceptance in the laser-based measurements community as more members of that community become proficient in its use and more familiar with the advantages of this method, which include lower costs, higher quality, and less time to achieve quantitative performance objectives.

Conclusion

We have applied modern design of experiments principles to a single-point laser based measurement apparatus for the first time at NASA Langley Research Center, and perhaps the first time outright. MDOE allowed us to scale the data volume to the customer's precision requirements. One consequence of this scaling was a large cost savings of perhaps a factor of five compared to previous measurements performed in the same facility. Another consequence of using MDOE was the minimization of systematic errors. This was achieved by randomizing the order of data acquisition as much as possible. Using MDOE allowed us to map the mean temperature with a 95% confidence level of ±30 K. This is substantially lower than the goal of ±50 K stated prior to the experiments. In fact, the precision requirements could have been achieved had the data volume been reduced by more than a factor of two.

We plan to more fully implement randomization in future experiments by redesigning the stepper-motor driven periscope system. Furthermore, we will investigate extending the analysis to fit CARS temperature maps in the third dimension (streamwise direction), creating an analytic model to predict the temperature in all three spatial coordinates within the duct. Another goal is to determine gas density from the intensity of the CARS signal. This is traditionally a difficult problem with CARS due to poor long-term optical stability, because drift in the system's alignment can cause an apparent decrease in measured density. MDOE's quality assurance tactics (randomization, replication, and blocking) are well suited to correct for this type of systematic bias error.

With minimal modification, the method outlined in this paper should be applicable to many other similar experimental methods, such as Rayleigh and Raman scattering experiments, laser-induced thermal grating (LITA) velocimetry, sound speed measurements, etc. It may even be possible to extend the method to imaging experiments, such as planar laser-induced fluorescence (PLIF), in an effort to improve measurement precision.

Acknowledgments

The experiments were carried out at NASA Langley Research Center in Hampton VA. We acknowledge the helpful contributions of Mr. Diego Capriotti, NASA Langley Research Center, for assistance in performing the experiments, and Dr. Sean O'Bryne of the National Research Council for helpful discussions.

References

1) Eckbreth, A. C. "Laser Diagnostics for Combustion Temperature and Species, " 2nd Ed., Gordon and Breach, 1996.

2) Fisher, R. A. "The Design of Experiments," 8th ed. Edinburgh: Oliver and Boyd. (1966).

3) Box, G. E. P., and N. R. Draper, "Empirical Model Building and Response Surfaces," New York, John Wiley and Sons, 1987.

4) Myers, R. H., and D. C. Montgomery, "Response Surface Methodology, Process and Product Optimization Using Designed Experiments," New York, John Wiley and Sons, 1995.

5) See for example, DeLoach, R. "Tactical Defenses Against Systematic Variation in Wind Tunnel Testing," AIAA Paper 2002-0885, 2002; DeLoach, R, J. S. Hill, W. G. Tomek, "Practical Applications of Response Surface Methods in the National Transonic Facility," AIAA Paper 2001-0167, 2001; DeLoach, R, "The Modern Design of Experiments: A Technical and Marketing Framework," AIAA Paper 2000-2691, 2000.

6) McClinton, C. R., S. M. Ferlemann, K. E. Rock, and P. G. Ferlemann, "The role of formal experiment design in hypersonic flight system technology development," AIAA Paper 2002-0543. 2002.

7) Ciancarelli, C. R., and K. M. Dorsett, "Optimizing the F-16 conformal fuel tank using design of experiments," AIAA Paper 2000-4522, 2000.

8) Parker, P., and R. DeLoach, "Structural optimization of a force balance using a

computational experiment design," AIAA Paper 2002-0540, 2002.

9) Snowdon, P., S. M. Skippon, and P. Ewart, "Improved precision of single-shot temperature measurements by broadband CARS by use of a modeless laser," Appl. Opt. 30, 1008-1010 (1991).

10) Hahn, J. W., C. W. Park, and S. N. Park, "Broadband coherent anti-Stokes Raman spectroscopy with a modeless dye laser," Applied Optics 36(27), 6722-6728, 1997.

11) Draper, N. R., and H. Smith, "Applied Regression Analysis," 2nd ed., New York, John Wiley and Sons, 1981.

12) Cutler, A. D., P. M. Danehy, R. R. Springer, R. DeLoach, and D. P. Capriotti, "CARS thermometry in a supersonic combustor for CFD code validation," AIAA-2002-0743, 2002.

13) O'Byrne, S., Private communication.

14) Drummond, J. P., G. S. Diskin, A. D. Cutler, and P. M. Danehy, "Fuel-Air Mixing and Combustion in Scramjets," AIAA Paper 2002-3878, July 2002.

15) Smith, M., R. Antcliff, A. Cutler, O. Jarrett, G. Northam, and D. Taylor, "CARS temperature measurements in a hydrogen-fueled supersonic combustor," AIAA Paper 90-5260, 1990.

16) Design-Expert®, Version 6.0.1, Stat-Ease, Inc., Minneapolis, MN, www.statease.com.

17) TableCurve®3D User's Manual, Version 3.0, © by AISN Software, Inc., 1997.